VILNIUS TECH
Vilnius Gediminas Technical University

Journal of Civil Engineering and Management
ISSN 1392-3730 / eISSN 1822-3605
2023 Volume 29 Issue 4: 318–328
https://doi.org/10.3846/jcem.2023.18597

MECHANICAL PROPERTIES OF A NEW FULLY PREFABRICATED STAGGERED FLIP-DOWN SLAB

Xuanqi RUAN[1], Deshen CHEN[2, 3*], Yan ZHANG[1, 2#], Zimeng HE[4], Yaning LI[2], Baiping AN[3]

[1]*College of Design and Engineering, National University of Singapore, Singapore, Singapore*
[2]*School of Ocean Engineering, Harbin Institute of Technology at Weihai, Weihai, China*
[3]*Tianyuan Construction Group Limited Company, Linyi, China*
[4]*Houston International Institute, Dalian Maritime University, Dalian, China*

Received 15 July 2022; accepted 22 November 2022

Abstract. Prefabricated slab has been widely used in the global construction industry due to energy saving, environmental protection, and good economic advantages. In this paper, a new type of fully prefabricated staggered flip-down slab without cast-in-situ operation has been proposed. First, the experiments were carried out on the new slab. The structural performance of the new slab was compared with the cast-in-situ slabs and composite slabs of the same specification. The experimental results showed that the ultimate bearing capacity of the new slab meets the requirements for practical utilization. On this basis, an additional CFRP sheet could be pasted on the bottom initial seam between prefabricated slabs to enhance the integrity and prevent cracks. Then, the whole loading process of the slab was simulated, and the results were consistent with the experimental results. Finally, through experiments and parametric analysis, recommendations for improvement were put forward to enhance the mechanical properties of this kind of slab.

Keywords: fully prefabricated staggered flip-down slab, bending test, mechanical properties, finite element analysis, parametric analysis.

Introduction

Prefabricated building systems are often referred to as precast constructions in which the structural components are manufactured in factories based on standardization, then transported to the sites, and finally assembled into the final product on the sites (Goodier & Gibb, 2007; Hassan et al., 2021). Because of prefabrication, the traditional execution of architectural design and construction is changed. Prefabricated buildings have been widely used and developed in the global construction industry due to their fast construction speed, site disruption reduction, sound economic benefits, better construction quality control, and improved material efficiency (Tam & Hao, 2014; Tam et al., 2007). In countries like Germany, New Zealand, and England, prefabrication accounts for 20%, almost 20% and around 10% of the total constructions, respectively (Heaton, 2017). Moreover, the proportion of new prefabricated dwellings in Japan has remained steady at 12–16% over the past decade (Steinhardt & Manley, 2016). In Sweden's housing industry, the market share of prefabricated construction has exceeded 80% (Navaratnam et al., 2019). In China, the government mandated that by 2020, 15% (by building slab area) of the nation's annual new construction should be prefabricated, and by 2025, this target is increased to 30% (State Council of the People's Republic of China, 2016).

A prefabricated slab is an important part of assembled residential buildings. It adopts the form of a precast panel plus a cast-in-situ layer. The precast panel can be used as a template to replace the bottom mold required by the cast-in-situ concrete floor (Xu et al., 2022). Although prefabricated slabs have the advantages of prefabricated structures, the inferior integral performance leads to poor seismic performance (Wang et al., 2019). In order to make the prefabricated slabs better meet the actual needs of the engineering project, experts and researchers have done many studies, and most have developed new types of slabs by improving the slab form. The ultimate bearing capacity of prefabricated steel-concrete composite slabs with an interlocking connection system proposed by Hassan et al. (2021) is 40% higher than that of the traditional

*Corresponding author. E-mail: *chends@hit.edu.cn*
#Corresponding author. E-mail: *zyrrm@outlook.com*

simply supported non-composite slabs. Lu et al. (2022) designed a prefabricated concrete composite slab that uses the profiled steel sheeting as prefabricated formwork and shear connectors, and experimentally evaluated its flexural performance in terms of reinforcement yield strength. Al-Fakher et al. (2021) demonstrated that the bearing capacity of a prefabricated concrete composite slab made with steel and composite reinforcing systems (CRS) reinforcement was increased by 112% when compared with the attachment of carbon fiber reinforced polymer sheets applied by Meng et al. (2016). Jiang et al. (2003) and Liu and Jiang (2004) proposed a composite slab with a precast inverted T-type bottom panel, which could improve the slab stiffness and integrity. Huang et al. (2015) concluded that the T-type ribs have almost no influence on the flexural performance of concrete composite slab with precast prestressed ribbed panel and suggested the calculation formulas for the cracking moment and ultimate bending moment. On this basis, Liu et al. (2020) presented a new prestressed concrete composite slab with precast inverted T-shaped ribbed panels (CSPRPs) and showed that different rib forms have little influence on the flexural behavior of CSPRPs. Chen et al. (2022) investigated a novel precast concrete slab with crossed bent-up rebar and showed that when the bend-up end angle of the slab was 60°, its flexural performance could be significantly improved. Nguyen et al. (2021) suggested hidden boundary one-way rib precast concrete slabs (HRS) and studied in detail the effects of strand wires and rebars on the bending performance of HRS.

The existing research studies show that the structural performance of slabs can be improved by changing the material while reducing the cost (Lukaszewska et al., 2010). By combining thin-walled cold-formed steel elements (CFS) and panels made of wood, cement, or plaster, de Seixas Leal and de Miranda Batista (2020) showed that the thin-walled channel shear connectors had excellent performance and could improve the bending capacity of the slab system. Mansour et al. (2015) found that adding a thin layer of steel fiber concrete into precast concrete slabs could increase its flexural performance. Dal Lago et al. (2017), Lima et al. (2018), and Crocetti et al. (2014, 2015) used fiber reinforcement in prefabricated concrete slabs and found that it has clear benefits on the post-cracking flexural capacity. May et al. (2019) studied the required load-bearing capacity and deflection stiffness of precast slabs made of carbon reinforced concrete at conventional construction height and demonstrated that the slab concrete could be reduced continuously by optimizing the load-bearing structure. Rochman et al. (2021) proved that lightweight foamed precast concrete slabs have good flexural behavior and can be used as a good prefabricated structural slab in the future. It can be seen from the literature review that the new slabs are mostly obtained by improving the form of composite slabs or changing materials, and the mechanical properties of slabs are explored through experiments and numerical simulation. However, the efficient assembly approach of slabs is rarely proposed.

In this paper, based on the survey of currently assembled slabs, a new fully prefabricated staggered flip-down slab with a high degree of prefabrication, good integrity, simple and reliable joint connections, no cast-in-situ operation, and low cost is developed. First, the bending test was carried out on the new slab. Then, its structural performance was compared with cast-in-situ and composite slabs of the same specification. The experimental results illustrate that the ultimate bearing capacity of the new slab meets the requirements for practical utilization. Further, the new slab was strengthened with the CFRP sheet to enhance the integrity of the initial seam between prefabricated slabs. Then, the whole loading process of the slab was simulated, and the results were found to be in good agreement with the experimental findings. Finally, through experiments and parametric analysis, some suggestions were presented to facilitate the construction and improve the mechanical properties of the slab.

1. Conceptual design

A fully prefabricated staggered flip-down slab is a new type of slab developed based on cast-in-situ and composite slabs. Figure 1 shows the specific form of the slab. After the plate is cut according to the modulus, the precast components with concave-convex grid-shaped tooth grooves are first produced in factories. Then, they form the prefabricated slab through staggered joints and buckles. Tensile and distribution reinforcements are embedded in the components, and the overlapping area between the top and bottom components is a quarter of the total area. In addition, the joint of the new slab is to put the two ends of the bottom prefabricated component on the steel beam, and the top part is staggered with the bottom. At the same time, the CFRP sheet can also be pasted on the bottom initial seam between prefabricated slabs to improve the integrity and prevent cracks.

Compared with other slabs, the new type of slab proposed in this paper has the following main advantages:

1) The presence of interlocking tooth grooves can improve the shear capacity and structural integrity;
2) The slab size has strong adaptability, so it can be transported conveniently;
3) Simple construction can improve assembly efficiency and advance the construction schedule; and
4) Compared with the traditional profiled steel plate composite slab, the flat slab surface can avoid suspended ceilings in decoration, leading to huge cost savings.

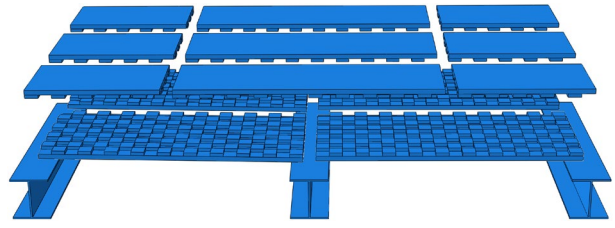

Figure 1. Slab specific form

2. Experimental design

2.1. Specimen design

In order to study the bending performance of the full prefabricated staggered flip-down slabs, six (6) slabs were designed in this experiment. The serial number and size of each specimen are shown in Table 1. The control group includes cast-in-situ slabs and composite slabs. Considering that the mechanical properties of the full prefabricated staggered flip-down slabs are smaller than those of cast-in-situ slabs and composite slabs in the same specification, additional control slabs with the thickness of 120 mm are set. The calculated span of each specimen is L_0 = 2200 mm. The HRB400 tensile and distribution reinforcements in all specimens adopt 4C8@150 and C6@200, respectively. The measured yield strength and tensile strength are f_y = 421 MPa and f_u = 647 MPa, while the elastic modulus is $E_s = 2\times10^5$ MPa. Moreover, each specimen uses C30 concrete. Figure 2 shows the design of the cast-in-situ slab and composite slab, while Figure 3 represents the design of the new fully prefabricated slab.

Slab ZPB consists of three components, i.e., one ZP-1 and two ZP-2. Figure 4 shows the production of ZP-1 and ZP-2. Considering that the new slab is fully assembled, one or two workers can carry out simple material transportation and slab installation. Their tooth grooves are designed as 150×150 mm with 40 mm height. The height of the bottom component is 55 mm. Slabs ZPB and ZPB-CFRP are equipped with the same reinforcement and concrete. CFRP can provide passive suppression for concrete and restrain the initial seam between prefabricated slabs, so the flexural capacity and stiffness of the slab can be improved.

Table 1. Specimen design

No.	Specimen	Designation	Thickness/mm	Length/mm	Width/mm
1	Fully prefabricated staggered flip-down slab	ZPB	150	2400	600
2	Fully prefabricated staggered flip-down slab with CFRP	ZPB-CFRP	150	2400	600
3	Cast-in-situ slab	XJB-150	150	2400	600
4		XJB-120	120	2400	600
5	Composite slab	DHB-150	150	2400	600
6		DHB-120	120	2400	600

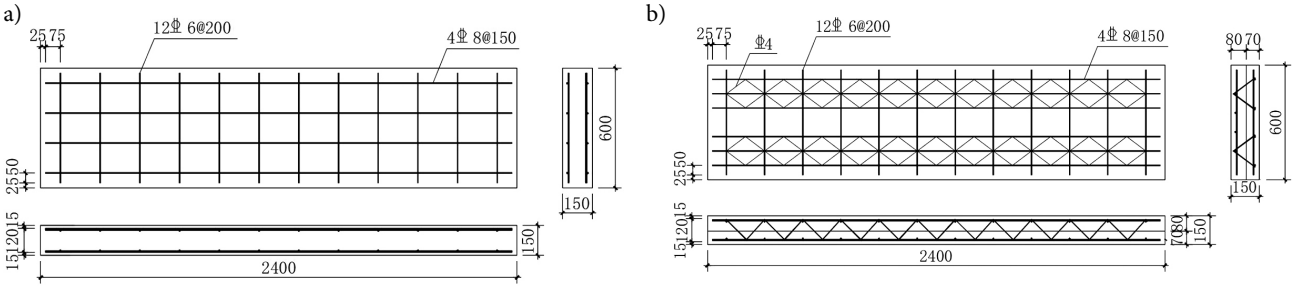

Figure 2. Design of the control group: a – cast-in-situ slab; b – composite slab

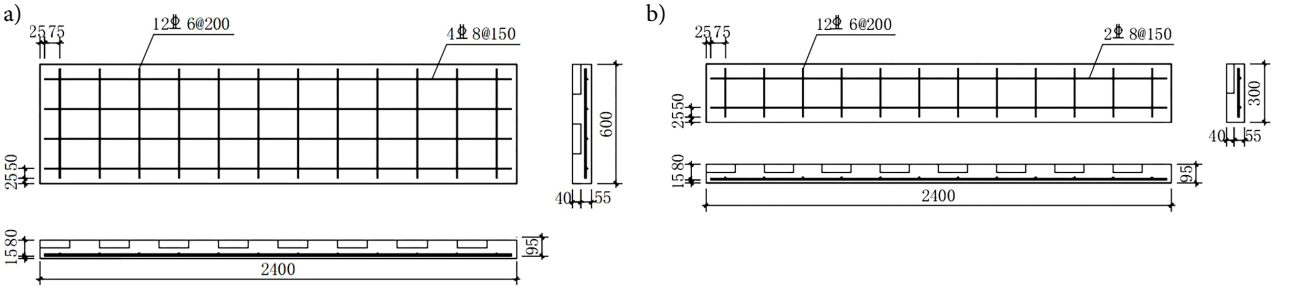

Figure 3. Design of the new fully prefabricated slab: a – ZPB-1; b – ZPB-2

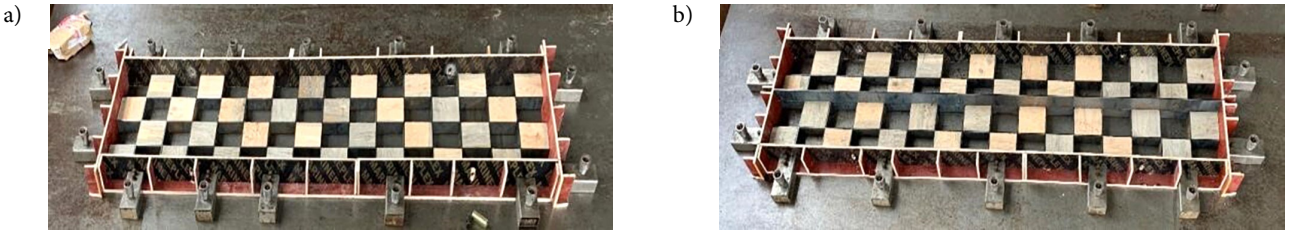

Figure 4. Production of ZPB: a – ZP-1; b – ZP-2

The position of the CFRP sheet is shown in Figure 5. The 200 mm CFRP sheet was pasted on longitudinal seam and extended to the edge of the supports. The tensile strength, elastic modulus, elongation at break, and thickness of CFRP sheet are f_u = 3870 MPa, E_s = 2.45×10^5 MPa, 1.74%, and 0.167 mm, respectively.

2.2. Experimental scheme

As shown in Figure 6, the specimen was loaded at three points. The preloading was divided into two steps. The load in each step was 2 kN, i.e., 50% of the cracking load. Each step lasted for 10 minutes for observation. Similarly, there were also two unloading stages. In formal loading, the stepped load was 2 kN until 8 kN. Then, it decreased to 1 kN when the cracking load reached and lasted until the first crack occurred. Next, the load increased by 2 kN every step before tensile reinforcement yielded. Finally, a 1 kN load lasted for the rest. The duration of every stage was 15 min to observe the experiment phenomenon and record it in detail. During the whole process, mid-span deflection, the strain in concrete, reinforcement, and CFRP sheet, and crack development should be concerned. Corresponding measuring points arranged are demonstrated in Figure 7 (Deflection: CD-1~CD-5, the strain of concrete: CS-1~CS-4, the strain of reinforcement: CX-1~CX-8, the strain of CFRP sheet: CFX-1~CFX~3).

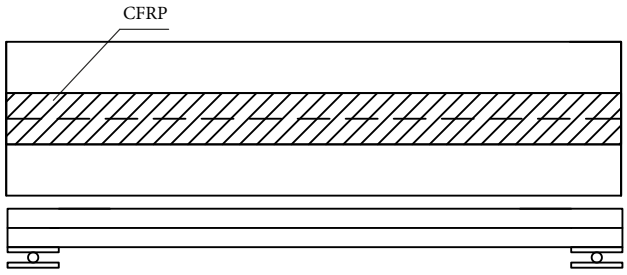

Figure 5. CFRP sheet

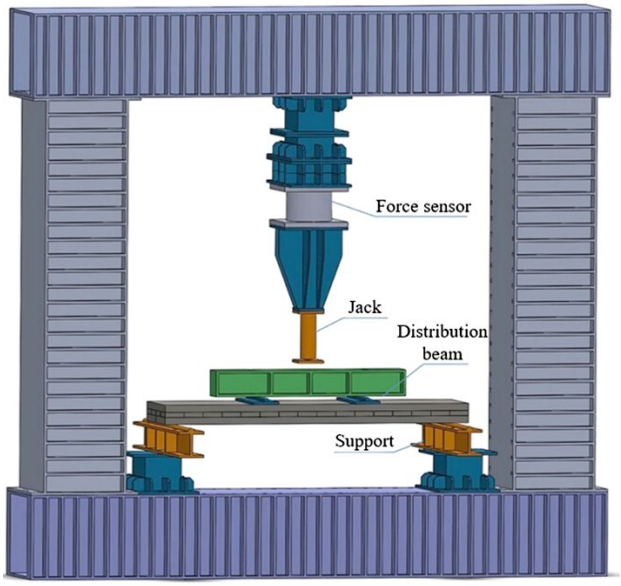

Figure 6. Loading mode

3. Experimental results

3.1. Bearing capacity analysis

Figure 8 shows the mid-span cracks of each specimen. The experimental phenomena, corresponding bearing capacity, and mid-span deflection in each stage are shown in Table 2, where P and u represent the load and deflection (the subscripts cr, y, and u represent the appearance of the first crack, and reaching yield and ultimate failure, respectively). The crack development of all specimens was similar. The representative bending test is illustrated in Figure 9. Taking ZPB as an example, the first tiny crack appeared when the load was 3 kN. The cracking load of ZPB was less than that of XJB or DHB because initial cracks existed at weak positions during installation. Then, new cracks developed in the mid-span at 12 kN, and some small cracks appeared near the supports at 20 kN. Next, the cracks extended upward and widened continuously until 32 kN when the maximum crack width of 1.5 mm reached the limit state, and the specimen failed. Compared with ZPB, due to the reinforcement effect of CFRP, the first crack, mid-span cracks, and cracks near the supports of ZPB-CFRP all appeared later. The slabs XJB, DHB, and ZPB, failed because the maximum crack width reached the limit state.

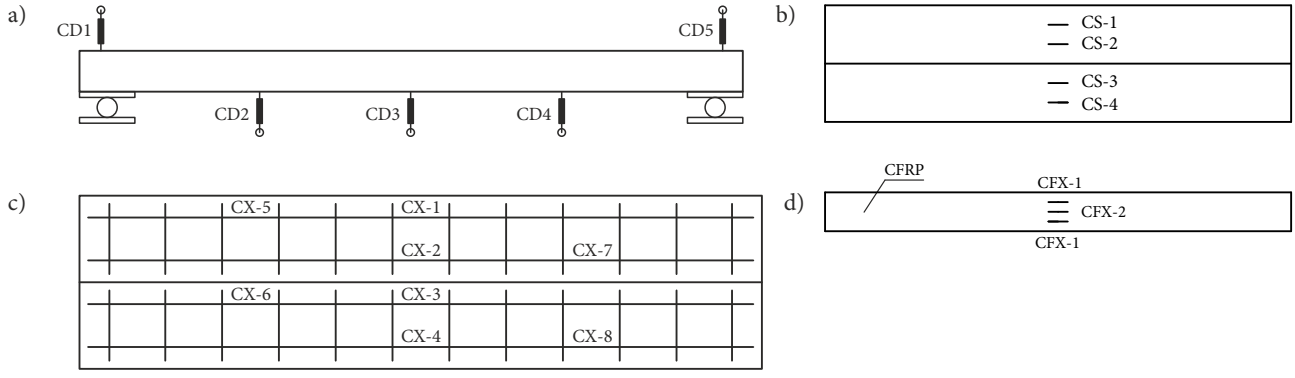

Figure 7. Arrangement of measuring points: a – measuring points arrangement of deflection; b – measuring points arrangement of the concrete strain gauge; c – measuring points arrangement of the steel strain gauge; d – measuring points arrangement of the CFRP strain gauge

Table 2. Experimental results and phenomena

Period	XJB-120	XJB-150	DHB-120	DHB-150	ZPB	ZPB-CFRP
P_{cr} (kN)/U_{cr} (mm) (First cracks appeared in mid-span)	6.20/1.62	9.35/0.89	8.20/0.95	10.00/0.70	3.00/0.50	7.50/0.78
P_y (kN)/U_y (mm)	19.40/15.33	30.25/14.43	19.83/11.47	30.24/13.70	29.53/15.85	35.65/16.72
P_u (kN)/U_u (mm) (Maximum crack width reaches the limit state of bearing capacity)	24.18/34.21	41.54/31.01	22.81/34.33	37.95/31.97	32.85/26.16	44.49/28.53
Failure mode	Maximum crack width reached the limit state					CFRP fractured

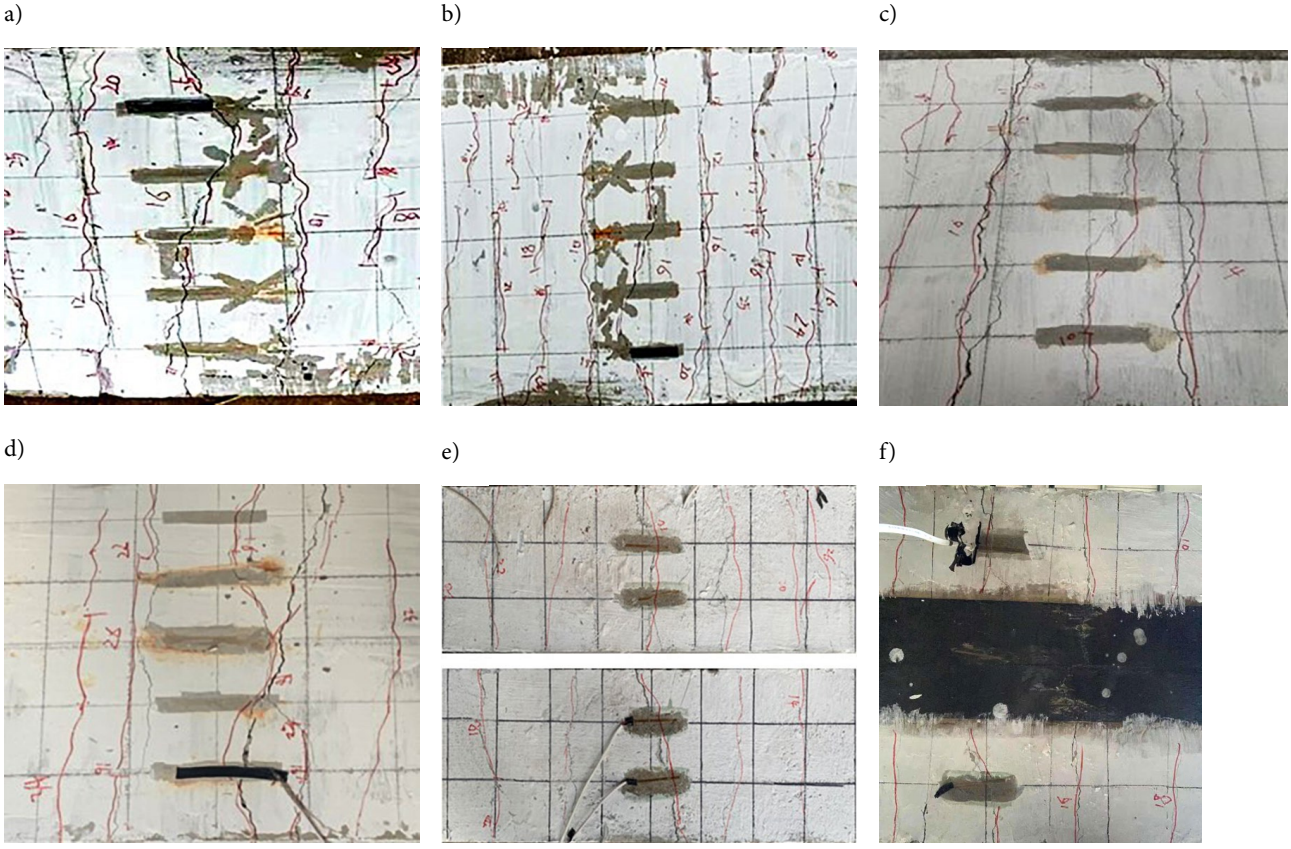

Figure 8. Mid-span cracks of each specimen: a – XJB-120; b – XJB-150; c – DHB-120; d – DHB-150; e – ZPB; f – ZPB-CFRP

There is no obvious cracking at the mid-span of the bottom of ZPB-CFRP, and the CFRP tensile fracture is taken as the limit state of ZPB-CFRP. However, as the load continued to increase, the reinforcement in the slab still had ductility and could continue to bear the tension force.

Figure 10 illustrates the relationship between the mid-span deflection of the slab and the external load. The initial stiffness and stiffness at the working stage (with cracks) of the composite slab are greater than that of the cast-in-situ slab due to a steel truss. However, because of inferior integrity, the ultimate bearing capacity of the composite slab is lower than that of the cast-in-situ slab. For ZPB and ZPB-CFRP, the tooth groove does not transfer internal force at the beginning of loading, and only the bottom component bears the load. Then, with increasing load, the mid-span deflection increases, and the top and bottom components slide, causing the tooth groove to squeeze each other and eliminate the gap between the tooth grooves. Because of the participation of the tooth groove, the bearing capacity of the slab will increase until the reinforcement yields. Further, the deflection of ZPB before the yield stage is larger than DHB-150, so its stiffness is lower than that of DHB-150. However, the ultimate bearing capacity of ZPB is about 86.6% of that of DHB-150, which meets the requirements for practical utilization. Also, the yield strength of ZPB-CFRP is the highest among all specimens. The reason is that CFRP bears tensile force and shows good anchorage and cementation effects in addition to reinforcement. Based on this, the ultimate bearing capacity of ZPB-CFRP increases by 17.2% and 35.4%, higher than that of DHB-150 and ZPB, respectively.

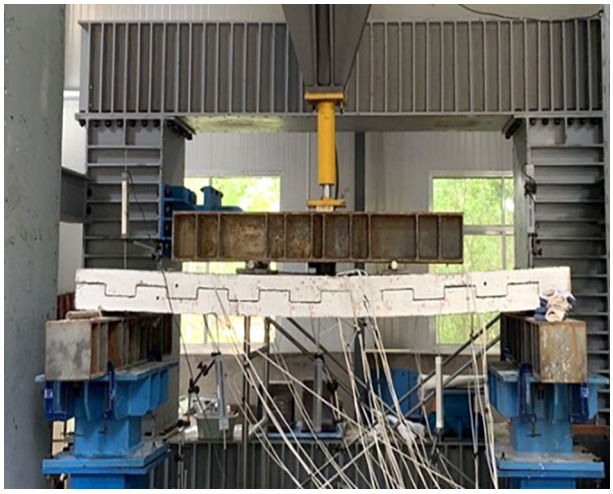

Figure 9. Bending test

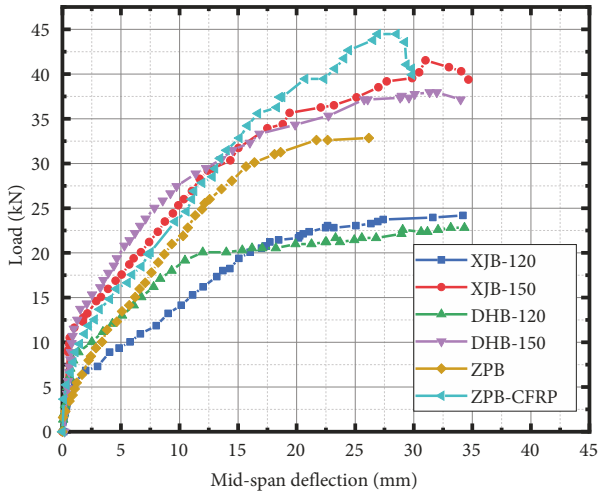

Figure 10. The relationship between mid-span deflection and external load

3.2. Load-strain curves analysis

As shown in Figure 11a, the load-strain curve of ZPB tensile reinforcement has the same trend as those of XJB and DHB, but the elastic stage for ZPB is short. It indicates that the concrete cracks when the load is not large, and its tensile part exits from work, thereby increasing stress in tensile reinforcement. Then, the strain of tensile reinforcement increases significantly with increasing load. In addition, it is worth mentioning that since the truss height adopted by DHB-150 is 90 mm, the top reinforcement is compressed first, and then the compressed reinforcement changes from compression to tension with the expansion of cracks. At the initial loading stage, due to the gaps between the tooth grooves, the top and bottom components of ZPB-CFRP work independently, so the strain of tensile reinforcement is small. However, as the load gradually increases, the top and bottom components slide and cause tooth grooves to squeeze each other and eliminate the gap, making ZPB-CFRP play a role as a whole. Therefore, the strain of tensile reinforcement in ZPB-CFRP is the largest under a large load. Figure 11b describes the load-strain curve of concrete in the compressive zone. The maximum strain of concrete in the compressive zone for six specimens was all within 3×10^{-3}, which did not reach the ultimate compressive strain of 3.3×10^{-3}. It is consistent with the phenomenon that the concrete was not crushed in the experiment.

4. Numerical simulations

4.1. Model development

To carry out numerical simulations for verifying experimental results and parametric analysis of fully prefabricated staggered flip-down slab, ABAQUS was used for modelling and simulating the loading process of ZPB and ZPB-CFRP. In the simulation process, the following assumptions were made in this study:

1) Reinforcement and concrete are closely integrated without relative slip, which accords with the coordination of displacement;

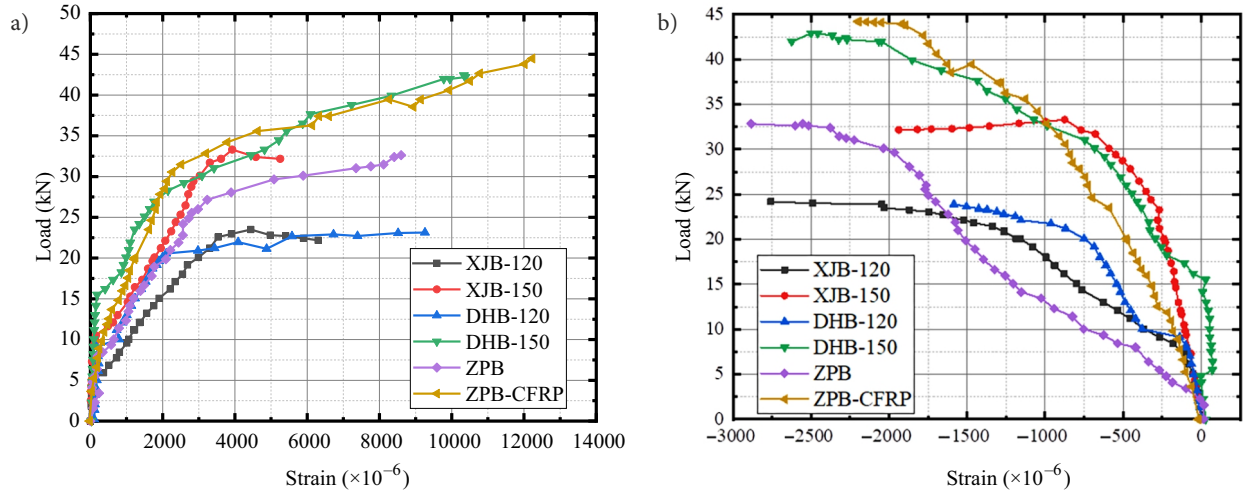

Figure 11. Load-strain curves: a – tensile reinforcement; b – compressive concrete

2) According to the experimental phenomena, there is no obvious slip between CFRP and slab, so it is assumed that CFRP and slab are closely combined without relative slip;
3) Although CFRP is an anisotropic material, the slab mainly relies on the CFRP sheet in a single direction in experiments. Hence, it is assumed that CFRP is a linear elastic material.

The mesh of slab components is shown in Figure 12. The basic mesh size was 50 mm, and local mesh refinement was conducted in the CFRP sheet. Brick element (C3D8R), truss element (T3D2), and membrane element (M3D4R) were used for concrete, reinforcement, and CFRP, respectively. The gap between the tooth grooves was 0.3 mm, and general contact was applied between the concrete components. The friction formula of the tangential behavior was the penalty function, and the friction coefficient was 0.55. The default setting was utilized for normal behavior. In order to facilitate the computation, the bilinear model and plastic damage model were utilized for constitutive relations by reinforcement and concrete, respectively. Poisson's ratios of concrete and steel were taken as 0.2 and 0.3. One end of the slab was considered fixed hinge support, while the other was the sliding hinge support.

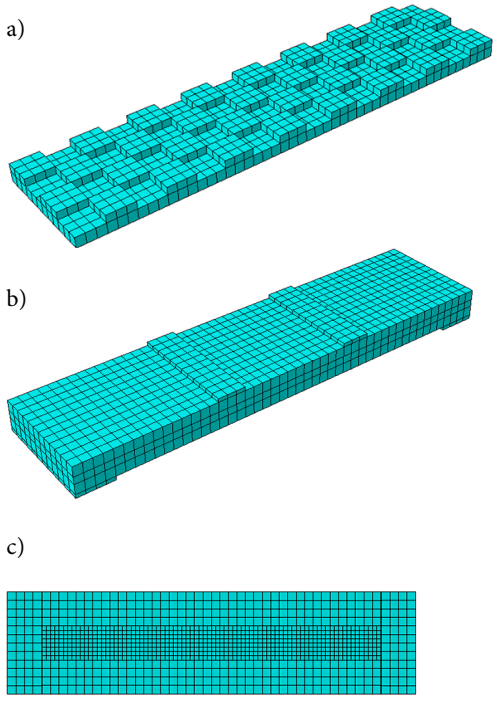

Figure 12. Modelling of the fully prefabricated staggered flip-down slab: a – component; b – overall model; c – CFRP

4.2. Comparison of results

In order to validate the feasibility and accuracy of the above finite element simulation method, the loading process of ZPB-CFRP was simulated and compared with the experimental results. As shown in Figure 13 and Table 3, the simulation results are consistent with the experimental results. The errors for yield deflection, ultimate strength, and ultimate deflection are all within 3%, and only the error for yield strength is 8.8%. The relative error may be caused due to the following reasons:

1) Ignoring the relative slip between reinforcement and concrete will lead to a larger calculation stiffness of the slab in simulations;
2) The plastic damage model is employed in simulations, simplifying the softening phenomenon of concrete after cracking;
3) The initial cracks caused during installation are not considered in the simulation process.

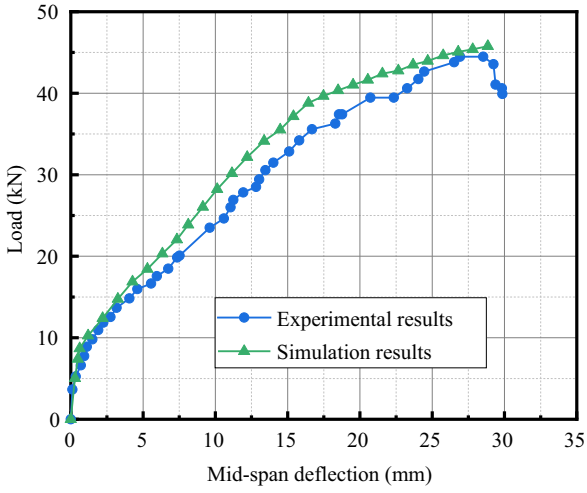

Figure 13. Comparison of the load-deflection curves

Table 3. Comparison of experimental and simulation results

Index	P_y	U_y	P_u	U_u
Experimental results	35.65 kN	16.72 mm	44.49 kN	28.53 mm
Simulation results	38.80 kN	16.44 mm	45.76 kN	28.84 mm
Error (%)	8.8	–1.7	2.9	1.1

Figure 14a shows the longitudinal stress of the bottom concrete. The tensile stress of concrete in the mid-span is the largest, so the slab is prone to crack in the mid-span. The high tensile stress zone extends from the mid-span to the supports, which corresponds to the experimental phenomenon of crack development. Moreover, it can be seen from Figure 14b that the high damage zone of the bottom concrete is distributed from mid-span to the loading point, and the maximum damage reaches 0.872. In the bending process, due to the mutual occlusion and extrusion between tooth grooves, it is easy to appear tensile damage in the tooth groove sides. Further, the longitudinal stress of the CFRP sheet is described in Figure 14c. In addition to reinforcement, the CFRP sheet al.o bears tensile force, which shows good anchorage and cementation effects. At the end of loading, the tensile stress of the CFRP sheet reaches the largest value of 1518 MPa.

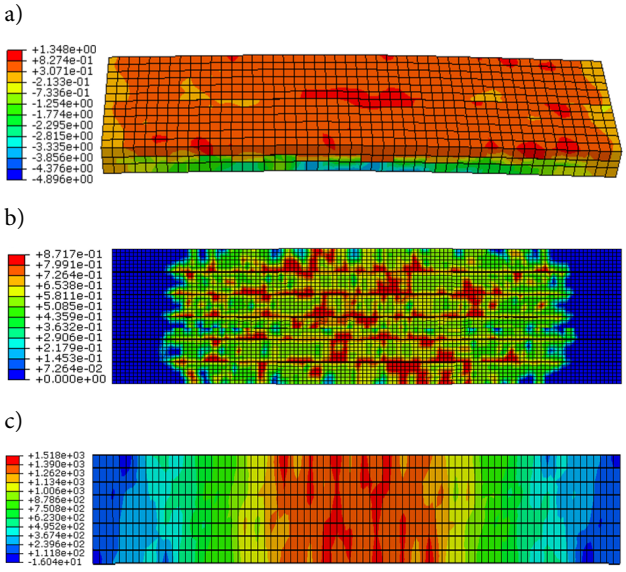

Figure 14. Simulation results of ZPB-CFRP: a – longitudinal stress of bottom concrete; b – tensile damage of bottom concrete; c – longitudinal stress of CFRP sheet

4.3. Analysis of key parameters

In order to identify the key factors affecting the mechanical properties of the slab, parametric analysis was carried out. The test conditions, including the slab thickness and CFRP width, are given in Table 4. Figure 15 shows the load-deflection curves under different test conditions. Test conditions 1, 2, and 3 illustrate that the slab thickness significantly influences the yield strength and ultimate strength because the effective height of the slab increases with increasing thickness. However, due to the influence of concrete strength and tensile reinforcement strength, thickness has little effect on cracking load. The ultimate strength of the slab with a thickness of 175 mm is 34.64% higher than that with a thickness of 150 mm. Compared to the 175 mm thick slab, the 200 mm thick slab has a 16.40% higher ultimate strength. It can be seen that the increase rate gradually decreases. Considering the principle of economy, the applicability of the structure, and construction standardization, after meeting the requirements of the bearing capacity of the slab, the slab thickness should be appropriately reduced to lower its dead weight and save materials. Therefore, under the same working conditions, for example, when the slab span is 3 m, it is recommended that the thickness of the new fully prefabricated slab be slightly greater than that of the cast-in-situ slab in practical applications, i.e., about 150 mm.

As shown in test conditions 1, 4, 5, and 6, the increase of CFRP width has little effect on the cracking load because concrete, reinforcement, and CFRP sheet bear the force together. In addition, since the CFRP sheet bears the tensile force, the neutral axis moves up slowly during the loading process, so the bearing capacity will become larger. The ultimate strength of the slab with 100 mm wide CFRP is 13.23% higher than that of the slab without CFRP pasting.

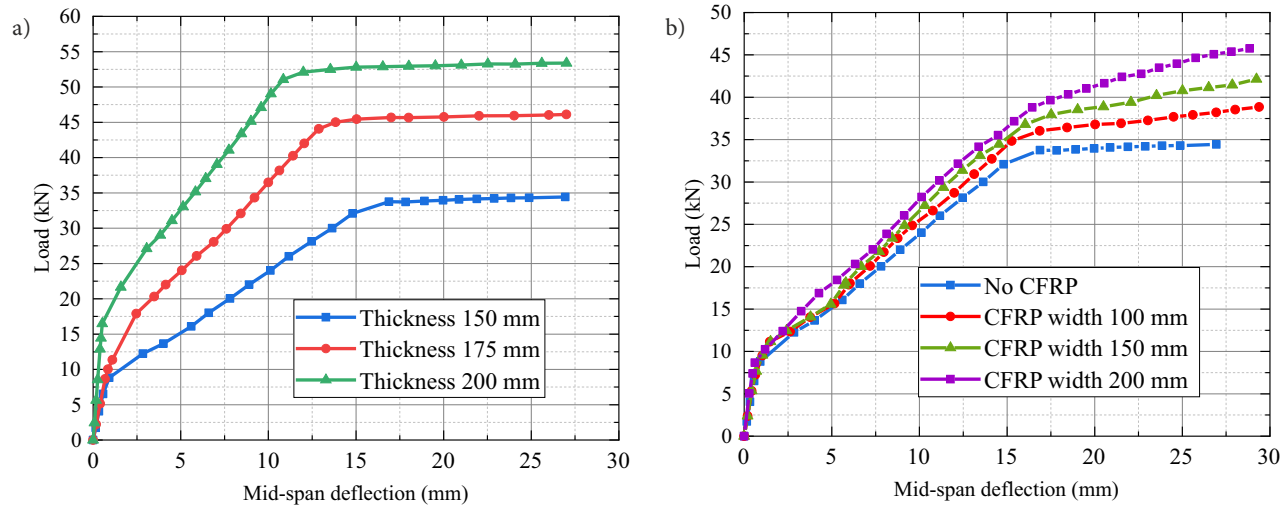

Figure 15. Load-deflection curves with different parameters: a – slab thickness; b – CFRP width

Table 4. Test conditions for slab thickness and CFRP width

Test condition	Thickness	CFRP width	Cracking load	Yield strength	Ultimate strength
1	150 mm	–	10.16 kN	33.21 kN	34.32 kN
2	175 mm	–	11.44 kN	44.21 kN	46.21 kN
3	200 mm	–	15.53 kN	51.31 kN	53.79 kN
4	150 mm	100 mm	10.59 kN	36.03 kN	38.86 kN
5	150 mm	150 mm	10.81 kN	36.94 kN	42.14 kN
6	150 mm	200 mm	11.05 kN	38.80 kN	45.76 kN

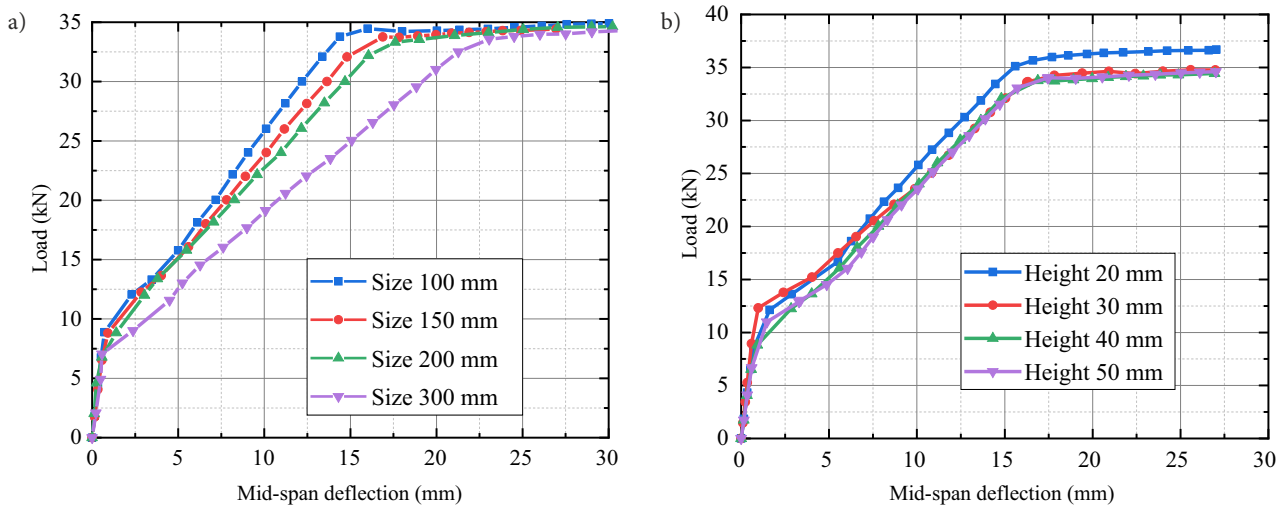

Figure 16. Load deflection curves with different parameters: a – tooth groove size; b – tooth groove height

Table 5. Test conditions for tooth groove size and height

Test condition	Tooth groove size	Tooth groove height	Cracking load	Yield strength	Ultimate strength
1	150×150 mm	40 mm	10.16 kN	33.21 kN	34.32 kN
7	100×100 mm	40 mm	10.28 kN	33.79 kN	34.81 kN
8	200×200 mm	40 mm	9.89 kN	33.08 kN	34.05 kN
9	300×300 mm	40 mm	9.56 kN	32.53 kN	33.77 kN
10	150×150 mm	20 mm	12.14 kN	35.09 kN	37.20 kN
11	150×150 mm	30 mm	12.05 kN	33.86 kN	34.96 kN
12	150×150 mm	50 mm	11.03 kN	33.07 kN	34.04 kN

From 100 mm to 200 mm, for every 50 mm increase in CFRP width, the ultimate strength of the slab rises by 8.44% and 8.59%, respectively, compared with the previous grade. The rate of increase gradually declines. To prevent the member from shear failure before flexural failure, the improvement of the flexural bearing capacity of the slab by CFRP reinforcement should not be too high. In practical application, it is recommended that the CFRP bonding area at the seam should account for 10–15% of the slab area.

Table 5 describes the test conditions for different sizes and heights of the tooth groove. The load-deflection curves of different test conditions are presented in Figure 16. The tooth groove size is related to the difficulty of template production and installation. It is of great significance to study the tooth groove size to improve construction efficiency and reduce resource waste. Moreover, the appropriate tooth groove height can reduce the structural weight. Test conditions 1, 7, 8, 9 and 1, 10, 11, 12 show that the size and height of the tooth groove have little effect on the bearing capacity of the slab. However, as the tooth groove size decreases, the corresponding deflection becomes smaller. Therefore, smaller tooth grooves can be selected in practical engineering.

Based on the experimental results and parametric analysis, the new slab can be optimized using the following approach. Since the stiffness of the new fully prefabricated slab is still inferior to that of the composite slab of the same specification after pasting the CFRP sheet on it, the tooth grooves can be improved by designing the contact surface between components as the inclined plane, thereby avoiding loose occlusion and enhancing the integrity of the fully prefabricated staggered flip-down slab. Furthermore, additional steel mesh can be configured on the side of tooth grooves to control the crack propagation.

Conclusions

In this paper, the investigations on the mechanical properties of a new type of fully prefabricated staggered flip-down slab were conducted through experimental analysis and simulations. The following conclusions are drawn from the obtained results:

1. A new, fully prefabricated, staggered flip-down slab was proposed for conceptual design. In production, there are no cast-in-situ operations for the new slab, and the bearing capacity is enhanced by tooth groove occlusion and staggered joint buckle. Furthermore, the CFRP sheet can be attached to the bottom initial seam between prefabricated slabs to improve the integrity and prevent cracks.
2. The stiffness of the new fully prefabricated slab before the yield stage is lower than that of a composite slab under the same thickness. However, its ultimate

bearing capacity is about 87% of that of the composite slab. Also, CFRP can improve the structural performance of the new slab. The yield strength of the new fully prefabricated slab with CFRP sheet is the highest among all specimens. Its ultimate bearing capacity is 17.2% and 35.4% higher than the composite slab and the new fully prefabricated slab, respectively.

3. The loading process of the new fully prefabricated slab and that with the CFRP sheet was simulated in ABAQUS. The simulation results were close to the experimental results, with a relative error of less than 10%. The failure process and crack development of the specimen were in good agreement.
4. It is recommended that the thickness of the new fully prefabricated slab be slightly greater than that of the cast-in-situ slab in practical engineering applications, for example, when the slab span is 3 m, the thickness of the new fully prefabricated slab is about 150 mm. The CFRP bonding area at the seam is suggested to account for 10–15% of the slab area. The slab can also adopt inclined tooth grooves for better integrity. Additional steel mesh can be arranged on the side of tooth grooves to control the crack propagation.

Funding

This work was supported by the China Postdoctoral Science Foundation under Grant number 2020M672132.

Author contributions

XR and DC conceived the study. XR, YZ and YL were responsible for the design and development of the data analysis. XR, ZH and YL were responsible for data collection and analysis. DC, YZ and YL were responsible for the experiments. XR, YZ and ZH were responsible for data interpretation. XR wrote the first draft of the article. DC was responsible for funding acquisition. DC and BA were responsible for supervision.

Disclosure statement

The authors declare that they have no conflict of interest. All the funding sources have been disclosed and are acknowledged in the manuscript.

References

Al-Fakher, U., Manalo, A., Ferdous, W., Aravinthan, T., Zhuge, Y., Bai, Y., & Edoo, A. (2021). Bending behaviour of precast concrete slab with externally flanged hollow FRP tubes. *Engineering Structures*, *241*, 112433. https://doi.org/10.1016/j.engstruct.2021.112433

Chen, Y., Shi, H., Wang, C., Wu, J., & Liao, Z. (2022). Flexural mechanism and design method of novel precast concrete slabs with crossed bent-up rebar. *Journal of Building Engineering*, *50*, 104216. https://doi.org/10.1016/j.jobe.2022.104216

Crocetti, R., Sartori, T., Tomasi, R., & Cabo, J. L. (2014). An innovative prefabricated timber-concrete composite system. In S. Aicher, H. W. Reinhardt, & H. Garrecht (Eds.), *RILEM bookseries: Vol. 9. Materials and joints in timber structures*. (pp. 507–516). Springer, Dordrecht. https://doi.org/10.1007/978-94-007-7811-5_47

Crocetti, R., Sartori, T., & Tomasi, R. (2015). Innovative timber-concrete composite structures with prefabricated FRC slabs. *Journal of Structural Engineering*, *141*(9), 04014224. https://doi.org/10.1061/(ASCE)ST.1943-541X.0001203

Dal Lago, B., Taylor, S. E., Deegan, P., Ferrara, L., Sonebi, M., Crosset, P., & Pattarini, A. (2017). Full-scale testing and numerical analysis of a precast fibre reinforced self-compacting concrete slab pre-stressed with basalt fibre reinforced polymer bars. *Composites Part B: Engineering*, *128*, 120–133. https://doi.org/10.1016/j.compositesb.2017.07.004

de Seixas Leal, L. A. A., & de Miranda Batista, E. (2020). Composite floor system with cold-formed trussed beams and prefabricated concrete slab: Selected and extended contribution of SDSS 2019. *Steel Construction*, *13*(1), 12–21. https://doi.org/10.1002/stco.201900046

Goodier, C., & Gibb, A. (2007). Future opportunities for offsite in the UK. *Construction Management and Economics*, *25*(6), 585–595. https://doi.org/10.1080/01446190601071821

Hassan, M. K., Subramanian, K. B., Saha, S., & Sheikh, M. N. (2021). Behaviour of prefabricated steel-concrete composite slabs with a novel interlocking system – numerical analysis. *Engineering Structures*, *245*, 112905. https://doi.org/10.1016/j.engstruct.2021.112905

Heaton, A. (2017, November 9). *Australia must break through prefabrication barriers*. Sourceable. https://sourceable.net/australia-must-break-through-prefabrication-barriers

Huang, H., Wu, F., Zhu, M., Zeng, C., & Lv, W. (2015). Influence of rib details on flexural behavior of concrete composite slab with precast prestressed ribbed panel. *Journal of Building Structures*, *36*(10), 66–72 (in Chinese). https://doi.org/10.14006/j.jzjgxb.2015.10.008

Jiang, Q., Wang, X., Liu, H., & Huang, S. (2003). Calculating method for bearing load capacity of RC invertible "T" slab-composite slab. *Journal of Central South University of Technology* (*Natural Science*), *34*(5), 567–570 (in Chinese). https://doi.org/10.3969/j.issn.1672-7207.2003.05.026

Lima, P. R., Barros, J. A., Roque, A. B., Fontes, C. M., & Lima, J. M. (2018). Short sisal fiber reinforced recycled concrete block for one-way precast concrete slabs. *Construction and Building Materials*, *187*, 620–634. https://doi.org/10.1016/j.conbuildmat.2018.07.184

Liu, H., & Jiang, Q. (2004). Experiment of inverted "T" simply supported composite slab. *Journal of Central South University* (*Science and Technology*), *35*(1), 147–150 (in Chinese). https://doi.org/10.3969/j.issn.1672-7207.2004.01.029

Liu, J., Hu, H., Li, J., Chen, Y. F., & Zhang, L. (2020). Flexural behavior of prestressed concrete composite slab with precast inverted T-shaped ribbed panels. *Engineering Structures*, *215*, 110687. https://doi.org/10.1016/j.engstruct.2020.110687

Lu, L., Ding, Y., Guo, Y., Hao, H., & Ding, S. (2022). Flexural performance and design method of the prefabricated RAC composite slab. *Structures*, *38*, 572–584. https://doi.org/10.1016/j.istruc.2022.02.022

Lukaszewska, E., Fragiacomo, M., & Johnsson, H. (2010). Laboratory tests and numerical analyses of prefabricated timber-concrete composite floors. *Journal of Structural Engineering*, *136*(1), 46–55. https://doi.org/10.1061/(ASCE)ST.1943-541X.0000080

Mansour, F. R., Bakar, S. A., Ibrahim, I. S., Marsono, A. K., & Marabi, B. (2015). Flexural performance of a precast concrete slab with steel fiber concrete topping. *Construction and Building Materials*, *75*, 112–120. https://doi.org/10.1016/j.conbuildmat.2014.09.112

May, S., Steinbock, O., Michler, H., & Curbach, M. (2019). Precast slab structures made of carbon reinforced concrete. *Structures*, *18*, 20–27. https://doi.org/10.1016/j.istruc.2018.11.005

Meng, X., Cheng, S., & El Ragaby, A. (2016). Experimental study on a novel shear strengthening technique for precast prestressed hollow-core slabs. In *Resilient infrastructure* (pp. STR-946-1–STR-946-9). London, UK.

Navaratnam, S., Ngo, T., Gunawardena, T., & Henderson, D. (2019). Performance review of prefabricated building systems and future research in Australia. *Buildings*, *9*(2), 38. https://doi.org/10.3390/buildings9020038

Nguyen, P. A., Kim, J., Oh, J., Park, Y., & Lee, D. (2021). Flexural behaviors assessment of Hidden boundary Rib precast concrete Slab (HRS) with bi-tensional prestress: Experiments, analyses, and formulations. *Structural Engineering and Mechanics*, *79*(6), 737–748. https://doi.org/10.12989/sem.2021.79.6.737

Rochman, T., Rasidi, N., & Purnomo, F. (2021). The flexural performance of lightweight foamed precast concrete slabs: Experimental and analysis. *GEOMATE Journal*, *20*(77), 24–32. https://doi.org/10.21660/2020.77.26463

State Council of the People's Republic of China. (2016). *Some opinions of the CPC Central Committee and the State Council on further strengthening the management of urban planning and construction* (in Chinese).

Steinhardt, D. A., & Manley, K. (2016). Adoption of prefabricated housing – the role of country context. *Sustainable Cities and Society*, *22*, 126–135. https://doi.org/10.1016/j.scs.2016.02.008

Tam, V. W., & Hao, J. J. (2014). Prefabrication as a mean of minimizing construction waste on site. *International Journal of Construction Management*, *14*(2), 113–121. https://doi.org/10.1080/15623599.2014.899129

Tam, V. W., Tam, C. M., & Ng, W. C. (2007). An examination on the practice of adopting prefabrication for construction projects. *International Journal of Construction Management*, *7*(2), 53–64. https://doi.org/10.1080/15623599.2007.10773102

Wang, Z., Li, P., & Tan, X. (2019). Advantages and disadvantages of prefabricated construction and improvement measures. *Sichuan Building Materials*, *45*(3), 39–40 (in Chinese). https://doi.org/10.3969/j.issn.1672-4011.2019.03.019

Xu, Q., Liu, J., & Li, N. (2022). Discussion on application of full precast slab in prefabricated high-rise residential buildings. *Guangdong Architecture Civil Engineering*, *29*(1), 35–38+69 (in Chinese). https://doi.org/10.19731/j.gdtmyjz.2022.01.009